Front. Phys. China, 2009, 4(2): 198–204
DOI 10.1007/s11467-009-0040-8

RESEARCH ARTICLE

Test of Lorentz invariance using optical cavities

Yan LI (李艳)[1,2], **Liu-feng LI** (李刘锋)[1,2], **Li-sheng CHEN** (陈李生)[1] (✉)

[1] *Wuhan Institute of Physics and Mathematics, Chinese Academy of Sciences, Wuhan 430071, China*
[2] *Graduate School of the Chinese Academy of Sciences, Beijing 100080, China*
E-mail: lchen@wipm.ac.cn

Received February 26, 2009; accepted March 2, 2009

This paper indroduces the precision test of Lorentz invariance using ultra-stable and low-loss optical cavities. The effective-field theory widely adopted in the analysis of experimental data has been reviewed. The sensitivity of the cavity resonant frequency to the Lorentz-violating tensor field is discussed in detail. In addition, the polarization of the optical field has been added to the model, and our analysis shows that the frequency shift due to Lorentz violation is not sensitive to the polarization of the optical field.

Keywords Lorentz invariance, spontaneous Lorentz violation, standard model extension

PACS numbers 03.03.+p, 03.70.+k, 04.20.-q, 07.60.-j

1 Introduction

The standard model of elementary particles has its foundations in quantum theory and special relativity. Over the past decades, theoretical and experimental investigations [1–4] have arrived at a regime where both quantum and relativity effects pervade, such as black holes and the dynamics of the early stage of the Universe [5, 6]. Although many progresses have been achieved, there are fundamental issues waiting for explanations, and a quantum theory of gravity is needed. The existing theory indicates that these two branches will merge at Planck scales (energy: 1.22×10^{28}eV, dimension: 1.61×10^{-35} m). To achieve this unification, many new theories beyond the standard model are under development. On the experimental side, tests of new theories down to the Planck scales are obviously unpractical. However, ongoing and planned precision measurements are able to search indirect evidences at low energies that point to new physics.

Being a symmetry of spacetime, Lorentz invariance is one of the founding pillars in Einstein's special relativity. In many developing new theories, this symmetry can be broken, opening possibilities of detectable effects at low-energy limits. For instance, in string theory there is a mechanism leading to a spontaneous break of Lorentz symmetry, and this effect may leave a low-energy signature [1, 2], which points a route for the test of quantum gravity at its low-energy limit.

This paper sketches the theoretical background and introduces the experimental test of Lorentz invariance using optical cavities. Section 2 concerns the theoretical background of the Lorentz symmetry break. The experimental test of Lorentz invariance using optical cavities is discussed in Section 3. This section begins with an introduction of the basic experimental setup, followed by a detailed review of the theoretical model that gives the relationship between the observation and various Lorentz-violating terms. In addition, the polarization dependence of the experiments is also examined.

2 Theory

2.1 Spontaneous Lorentz violation

We generally expect that the Lorentz violation arises from a spontaneous symmetry break. In this mechanism the symmetry of the original Lagrangian and the dynamics is not explicitly violated, but the ground state of the system fails to respect the symmetry. The central idea of the spontaneous symmetry broken is that a field acquires a nonzero vacuum expectation value (VEV) and can couple to other fields. For instance, the Higgs field with a nonzero VEV generates a spontaneous symmetry break in the standard model based on a $SU(2)\times U(1)$ symmetry. In string theory there is a possibility that the Lorentz symmetry can be spontaneously broken [1]. This

approach allows for tensor fields having nonzero VEVs and definite space-time orientations. Thus the Lorentz symmetry can be violated for known fields because of their interactions with the tensor fields. For example, in the Bumblebee model, tensor field B^μ acquires a nonzero VEV b^μ:

$$L_B = L_g + L_{gB} + L_k + L_\nu + L_J \tag{1}$$

where L_g is the Lagrangian of the gravitational field, L_{gB} is the interaction between the tensor field and gravitational field, L_k is the kinetic energy of the tensor field, L_ν contains potential energy that leads to spontaneous Lorentz violation, and L_J denotes the interaction with other fields.

Although the analysis based on spontaneous symmetry break allows a close examination of the properties of the Lorentz violation, it has limited application in the experimental test of Lorentz invariance because the explicit form of the resultant Largrangian varies with different scenarios of the spontaneous Lorentz violation. Alternatively, an effective Largrangian has been developed to encompass a complete set of possible Lorentz-violating terms that may have different origins, including spontaneous symmetry break. The following section gives a brief review of this effective field theory.

2.2 Effective-field theory

Alternatively, Lorentz violation can also be described by an effective-field theory, which is often employed to extract the upper bounds from experimental data for various Lorentz-violating terms in different particle sectors. In effective-field theory various Lorentz-violating terms are added into the original standard model Lagrangian. The theory can be viewed as a phenomenological theory describing Lorentz violation as:

$$L = L_{SM} + \delta L \tag{2}$$

where δL contains the interaction between standard-model fields and the gravitational field. In this effective-field theory, physical results are still independent of the observer; i.e., the observer symmetry is preserved. Effective-field theory with observer-independent Lorentz-violating terms is called standard model extension (SME). To guarantee observer independence, δL can only contain observer scalars under local Lorentz and general coordinate transformations:

$$T_{\lambda\mu\nu\ldots}(SM)^{\lambda\mu\nu\cdots} \subseteq \delta L \tag{3}$$

Note that the gravitational field has been included in tensor field $T_{\lambda\mu\nu\ldots}$. The relationship between $T_{\lambda\mu\nu\ldots}$ and $T_{abc\ldots}$ in a local Lorentz frame is [7]

$$T_{\lambda\mu\nu\ldots} = e^a_\lambda e^b_\mu e^c_\nu \cdots T_{abc\ldots} \tag{4}$$

where e^a_λ provides the link between the spacetime manifold and local Lorentz frame, and satisfies $g_{\mu\nu} = e^a_\lambda e^b_\mu \eta_{ab}$ ($g_{\mu\nu}$ and η_{ab} are the metrics of the spacetime manifold and local Lorentz frame, respectively). The covariant derivatives including spin connection $\omega^a_{\mu b}$ are

$$D_\mu e^a_\nu = \partial_\mu e^a_\nu - \Gamma^\alpha_{\mu\nu} e^a_\alpha + \omega^a_{\mu b} e^b_\nu \tag{5}$$

In the Minkowski limit, $g_{\mu\nu} = \eta_{\mu\nu}$ and $T_{\lambda\mu\nu\ldots}$ becomes a constant tensor in a fixed frame.

In principle, SME contains an infinite number of terms. To investigate the low-energy effect, a subset of the SME, namely, the minimal SME, only considers those terms with power-counting renormalizability and gauge invariance. The minimal SME of QED is [8, 9]

$$\begin{aligned} L = {} & \frac{\mathrm{i}}{2}\bar{\psi}\Gamma_\nu D^\nu \psi - \frac{1}{2}\bar{\psi}M\psi - \frac{1}{4}F^{\mu\nu}F_{\mu\nu} \\ & -\frac{1}{4}(k_F)_{\kappa\lambda\mu\nu}F_{\kappa\lambda}F_{\mu\nu} + \frac{1}{2}(k_{AF})^\kappa \varepsilon_{\kappa\lambda\mu\nu}A^\lambda F^{\mu\nu} \end{aligned} \tag{6}$$

where

$$\begin{aligned} \Gamma_\nu &= \gamma_\nu + c_{\mu\nu}\gamma^\mu + d_{\mu\nu}\gamma_5\gamma^\mu + e_\nu + \mathrm{i}f_\nu\gamma_5 + \frac{1}{2}g_{\lambda\mu\nu}\sigma^{\lambda\mu} \\ M &= m + a_\mu\gamma^\mu + b_\mu\gamma_5\gamma^\mu + \frac{1}{2}H_{\mu\nu}\sigma^{\lambda\mu} \end{aligned} \tag{7}$$

$c_{\mu\nu}$, $d_{\mu\nu}$, e_ν, f_ν, $g_{\lambda\mu\nu}$, a_μ, b_μ, $H_{\mu\nu}$, $(k_F)_{\kappa\lambda\mu\nu}$, $(k_{AF})^\kappa$ are tensors responsible for Lorentz violation. The last two terms in the Lagrangian originate from the photon sector, and the rest are from electron sector.

In this effective-field theory, Lorentz violation happens in the form of a particle symmetry break, meaning physical results change as a transformation (such as translation or rotation) is performed upon the particles. As shown in Fig. 1, $T_{\lambda\mu\nu\ldots}$ can be viewed as a nonzero background tensor field, which bears spacetime indices and specifies a spacetime direction. Lorentz violation is thus possible because of the new interaction between the particle and the tensor field.

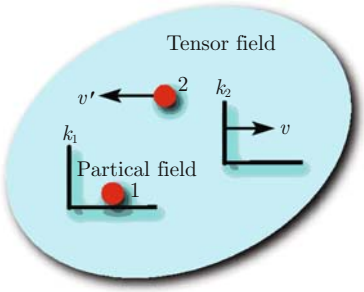

Fig. 1 Effective-field theory of Lorentz violation. Inertial frame $k_1$is at rest with respect to a tensor field while inertial frame k_2 moves. Two observers, standing still, respectively, in k_1 and k_2, perform the same measurements on a particle (particle 1) that is at rest in frame k_1. Their results are related to each other according to Lorentz transformation; thus, the observer symmetry is preserved. However, if the particle moves with respect to the tensor field (particle 2), Lorentz symmetry can be broken because of the new interaction between the particle and the tensor field.

3 Experimental test of Lorentz symmetry using optical cavities

3.1 Modification of the resonant frequency of an optical cavity due to Lorentz violation in the context of SME

Lorentz violation in electrodynamics can be tested with high precision using microwave [10] or optical cavities [11]. We now introduce the experimental test of the Lorentz invariance using optical cavities in the context of SME. Figure 2 is the basic experimental setup.

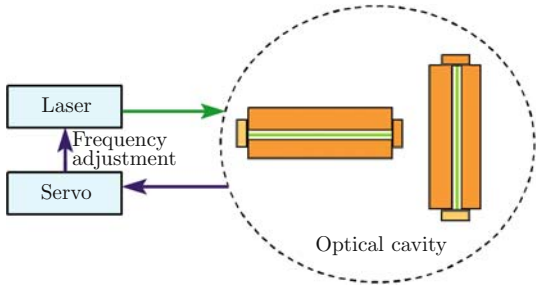

Fig. 2 Test of Lorentz invariance using optical cavities. Two separate laser beams are independently locked to two cavities that are orthogonal to each other in the horizontal plane. The cavities are either fixed in the lab frame or installed on a turntable.

The resonant frequency of an optical cavity is

$$\omega = 2\pi\frac{mc}{2nL} \tag{8}$$

where m is an integer, c is the speed of light in vacuum, n is the refractive index of the cavity filling material, and L is the cavity length. Hereinafter, we focus on empty cavities whose optical path is void of matter. The resonant frequency of the cavity is modified via three pathways if there is a genuine Lorentz violation:

(1) Lorentz violation in the photon sector will change the resonant frequency of the cavity. This could be attributed to a small modification of the speed of light in vacuum ($c = c_0+\delta c$) because of the photonic Lorentz violation [12],

$$\frac{\delta c}{c_0} = \frac{1}{2}[(\hat{N}\times\hat{E}^*)\kappa_{HB}(\hat{N}\times\hat{E}) - \hat{E}^*\kappa_{DE}\hat{E}] \tag{9}$$

Here, the unit vectors $\boldsymbol{N}$ and $\boldsymbol{E}$, respectively, denote the directions of the cavity axis and the polarization. κ_{DE},κ_{HB}, κ_{DB}, and κ_{HE} are defined through

$$(\kappa_{DE})^{jk} = -2(k_F)^{0j0k}, (\kappa_{HB})^{jk} = \frac{1}{2}\varepsilon^{jpq}\varepsilon^{krs}(k_F)^{pqrs}$$
$$(\kappa_{DB})^{jk} = -(\kappa_{HE})^{kj} = \varepsilon^{kpq}(k_F)^{0jpq} \tag{10}$$

(2) Photonic Lorentz violation also modifies the Coulomb potential $\Phi(\boldsymbol{x}) = \dfrac{e^2}{4\pi|\boldsymbol{x}|} + V(\boldsymbol{x})$, changing the length of the cavity in the following way [13]:

$$\frac{\delta L}{L} = a_{/\!/}\hat{N}(\kappa_{DE})_{\rm lab}\hat{N} + a_\perp[\hat{E}^*(\kappa_{DE})_{\rm lab}\hat{E} + (\hat{N}\times\hat{E}^*)(\kappa_{DE})_{\rm lab}(\hat{N}\times\hat{E})] \tag{11}$$

The values of $a_{/\!/}$ and $a_\perp$ are related to the material properties of the cavity. Detailed analysis indicates this effect is negligible for most experiments [13].

(3) Electronic Lorentz violation modifies the kinetic energy of an electron, leading again to a change in the cavity length [14, 15]. The strain tensor of the cavity material related to this effect is

$$e_{jk} = \frac{1}{2}\left(\frac{\partial L_j}{\partial x_k} + \frac{\partial L_k}{\partial x_j}\right) = B_{jklm}E'_{lm} \tag{12}$$

Here, $E'_{jk} = -c_{jk} - \dfrac{1}{2}c_{00}\delta_{jk}$. B is the sensitivity tensor solely determined by the material properties of the cavity. It is then straightforward to determine the length change from e_{jk} using the standard strain-stress relationship in a continuum. As an example, the nonzero elements of the sensitivity tensor for cubic crystals or noncrystalline materials are listed below:

$$\begin{aligned}
&B_{1111} = B_{2222} = B_{3333} = B_{11}\\
&B_{1122} = B_{1133} = B_{2211} = B_{2233}\\
&\qquad = B_{3311} = B_{3322} = B_{12}\\
&B_{1133} = B_{2233} = B_{13}\\
&2B_{2323} = 2B_{3131} = 2B_{1212} = B_{44}
\end{aligned} \tag{13}$$

Combining the abovementioned three effects, one obtains the frequency shift induced by Lorentz violation in electrodynamics:

$$\frac{\delta\nu}{\nu} = \frac{\delta c}{c_0} - \frac{\delta L}{L} \tag{14}$$

3.2 Resonant frequency shift of an optical cavity with specified orientation and polarization

Here, we assume that the cavity axis is in the x-y plane: $\hat{N} = (\cos\theta, \sin\theta, 0)$ and the polarization of the light $\hat{E}_0$, being perpendicular to $\hat{N}$ has an angle δ with respect to the z axis: $\hat{E}_0 = (\sin\delta\sin\theta, -\sin\delta\cos\theta, \cos\delta)$. The frequency shift due to photonic and electronic Lorentz violations can be organized to

$$\frac{\delta\nu}{\nu} = A + B\sin\theta + C\cos\theta + D\sin 2\theta + E\cos 2\theta \tag{15}$$

with

$$\begin{aligned}
A = -\frac{1}{4}[&(\kappa_{DE})^{11}_{\rm lab}\sin^2\delta + (\kappa_{DE})^{22}_{\rm lab}\sin^2\delta\\
&+2(\kappa_{DE})^{33}_{\rm lab}\cos^2\delta - (\kappa_{HB})^{11}_{\rm lab}\cos^2\delta\\
&-(\kappa_{HB})^{22}_{\rm lab}\cos^2\delta - 2(\kappa_{HB})^{33}_{\rm lab}\sin^2\delta] + B_{12}\cdot E'^{33}_{\rm lab}
\end{aligned}$$

$$+\frac{1}{2}(B_{11}+B_{12})\cdot(E'^{11}_{\rm lab}+E'^{22}_{\rm lab})$$

$$B=-[(\kappa_{DE})^{13}_{\rm lab}+(\kappa_{HB})^{13}_{\rm lab}]\sin\delta\cos\delta$$

$$C=[(\kappa_{DE})^{23}_{\rm lab}+(\kappa_{HB})^{23}_{\rm lab}]\sin\delta\cos\delta$$

$$D=\frac{1}{2}[(\kappa_{DE})^{12}_{\rm lab}\sin^2\delta-(\kappa_{HB})^{12}_{\rm lab}\cos^2\delta]$$
$$-\frac{1}{2}(B_{11}-B_{12})\cdot E'^{12}_{\rm lab}-\frac{1}{2}(B_{11}-B_{12})\cdot E'^{21}_{\rm lab}$$

$$E=\frac{1}{4}[((\kappa_{DE})^{11}_{\rm lab}-(\kappa_{DE})^{22}_{\rm lab})\sin^2\delta-((\kappa_{HB})^{11}_{\rm lab}$$
$$-(\kappa_{HB})^{22}_{\rm lab})\cos^2\delta]+\frac{1}{2}(B_{11}-B_{12})\cdot E'^{11}_{\rm lab}$$
$$-\frac{1}{2}(B_{11}-B_{12})\cdot E'^{22}_{\rm lab} \quad (16)$$

A varying frequency shift can be interpreted as an experimental evidence of Lorentz violation when the test is performed in a boosted/rotated coordinate. Often the cavity is fixed in a laboratory frame that moves with the Earth's rotation and orbit, as shown in Fig. 3. In addition, the cavity can be installed on a turntable with its rotational axis around $z_{\rm lab}$ and an angular frequency of ω_l. In the framework of SME, the upper bounds of various Lorentz-violating terms can be extracted from the experimental data with the help of Eqs. (15) and (16).

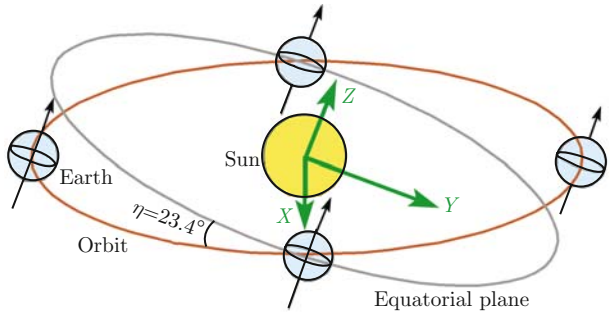

Fig. 3 Sun-centered coordinate. η=23.4° is the angle between the orbital and equatorial planes

3.3 Lorentz-violating parameters in Sun-centered frame

In order to use the rotational and orbital movements of the Earth, we transform the tensor from the lab frame to the Sun-centered frame, i.e.,

$$T^{\lambda\mu\nu\cdots}_{lab}=\Lambda^{\lambda}_{a}\Lambda^{\mu}_{b}\Lambda^{\nu}_{c}\cdots T^{abc\cdots}_{\rm Sun} \quad (17)$$

The explicit form of the matrix Λ is listed in Appendix 1. With Eq. (17), one can derive the following transformations for the related Lorentz-violating parameters:

$$(\kappa_{DE})^{jk}_{\rm lab}=T^{jkJK}_{0}(\kappa_{DE})^{JK}-T^{(jk)JK}_{1}(\kappa_{DB})^{JK}$$
$$(\kappa_{HB})^{jk}_{\rm lab}=T^{jkJK}_{0}(\kappa_{HB})^{JK}-T^{(jk)KJ}_{1}(\kappa_{DE})^{JK}$$
$$(\kappa_{DB})^{jk}_{\rm lab}=T^{jkJK}_{0}(\kappa_{DB})^{JK}+T^{kjJK}_{1}(\kappa_{DE})^{JK}$$
$$+T^{jkJK}_{1}(\kappa_{HB})^{JK} \quad (18)$$

$$c^{00}_{\rm lab}=-\beta^{J}(c^{TJ}+c^{JT})$$
$$c^{ij}_{\rm lab}=-R^{ik}R^{jJ}\beta^{k}c^{TJ}-R^{jk}R^{IJ}\beta^{k}c^{JT}$$
$$+R^{iI}R^{jJ}c^{IJ} \quad (19)$$

Here, $T^{jkJK}_{0}=R^{jJ}R^{kK}$, $T^{jkJK}_{1}=R^{jP}R^{kJ}\varepsilon^{KPQ}\beta^{Q}$, and R is the rotation matrix. Note that in obtaining the above transformation, the quadratic and higher-order terms in β have been dropped. In order to analyze the result more conveniently, we make the following decomposition [12]:

$$(\tilde{\kappa}_{e+})^{JK}=\frac{1}{2}(\kappa_{DE}+\kappa_{HB})^{JK}$$
$$(\tilde{\kappa}_{e-})^{JK}=\frac{1}{2}(\kappa_{DE}-\kappa_{HB})^{JK}-\frac{1}{3}\delta^{JK}(\kappa_{DE})^{LL}$$
$$(\tilde{\kappa}_{o+})^{JK}=\frac{1}{2}(\kappa_{DB}+\kappa_{HE})^{JK}$$
$$(\tilde{\kappa}_{o-})^{JK}=\frac{1}{2}(\kappa_{DB}-\kappa_{HE})^{JK}$$
$$\tilde{\kappa}_{tr}=\frac{1}{3}(\kappa_{DE})^{LL} \quad (20)$$

where $\tilde{\kappa}_{o+}$ is antisymmetric and the others are symmetric. $\tilde{\kappa}_{tr}$ is a scalar. This new combination is more convenient to analyze the sensitivity of the Lorentz-violating parameters in the experiment. Analysis of the astrophysical data shows $\left|(\tilde{\kappa}_{e+})^{JK}\right|,\left|(\tilde{\kappa}_{o-})^{JK}\right|\leqslant 10^{-32}$(Sun-centered frame) [12]. As a result, these two sets of parameters can be neglected with the present experimental precision. The final result can be written as:

$$A=A_0+A_{s1}\sin\omega_{\oplus}T_{\oplus}+A_{c1}\cos\omega_{\oplus}T_{\oplus}+A_{s2}\sin2\omega_{\oplus}T_{\oplus}$$
$$+A_{c2}\cos2\omega_{\oplus}T_{\oplus}$$
$$B=B_0+B_{s1}\sin\omega_{\oplus}T_{\oplus}+B_{c1}\cos\omega_{\oplus}T_{\oplus}$$
$$+B_{s2}\sin2\omega_{\oplus}T_{\oplus}+B_{c2}\cos2\omega_{\oplus}T_{\oplus}$$
$$C=C_0+C_{s1}\sin\omega_{\oplus}T_{\oplus}+C_{c1}\cos\omega_{\oplus}T_{\oplus}$$
$$+C_{s2}\sin2\omega_{\oplus}T_{\oplus}+C_{c2}\cos2\omega_{\oplus}T_{\oplus}$$
$$D=D_0+D_{s1}\sin\omega_{\oplus}T_{\oplus}+D_{c1}\cos\omega_{\oplus}T_{\oplus}$$
$$+D_{s2}\sin2\omega_{\oplus}T_{\oplus}+D_{c2}\cos2\omega_{\oplus}T_{\oplus}$$
$$E=E_0+E_{s1}\sin\omega_{\oplus}T_{\oplus}+E_{c1}\cos\omega_{\oplus}T_{\oplus}$$
$$+E_{s2}\sin2\omega_{\oplus}T_{\oplus}+E_{c2}\cos2\omega_{\oplus}T_{\oplus} \quad (21)$$

The signal contains fundamental and second harmonic of the Earth's rotational frequency, while the comparatively slow orbital dependence is absorbed by the fitting parameters on the right-hand side of Eq. (21). The explicit forms of these fitting parameters are listed in Appendix 2. The final result is independent of δ, indicating that the result is not sensitive to the polarization of the light. This analysis can be easily extended to the case of

two orthogonal cavities, as shown in Fig. 2.

4 Summary and remarks

A precision test of Lorentz invariance can be implemented by ultra-stable and low-loss optical cavities. The effective-field theory widely adopted in this type of experiment has been reviewed. The sensitivity of the cavity resonant frequency to the Lorentz-violating tensor field is discussed in detail. In addition, the polarization of the optical field has been added to the model, and our analysis shows that the frequency shift due to Lorentz violation is not sensitive to the polarization of the optical field.

A complementary task is to investigate how Lorentz symmetry is preserved with high precision in the low-energy limit readily accessed by the experiments while, in new theories, the symmetry can break at high energies. Addressing this "fine-tuning" problem becomes more urgent as the upper bounds of various Lorentz-violating terms have been continuously pushed down by laboratory precision measurements [16−22], high-energy particle physics [23−25], and astronomical observations [26−28].

Unexplained physical phenomena in different branches can share the same origin when examined in a deeper theory. Extensive and detailed experimental data are needed to cast a web of connection on a variety of ongoing precision measurements from which new theory can be extracted and distilled. That direct theoretical predications are only available down to the Planck scale is an obstacle confronting current experiments. High-energy particle physics and astronomical observations are major ways to probe the fundamental laws of physics. Besides, large-scale ground-based or space-born precision measurements and controlled experiments in laboratories can also provide complementary tests aiming at an exhaustive search for the signatures of new theories. With the continuously improved precision, hope does exist to bridge the gap between the new theories and their direct experimental verification.

Acknowledgements This work was supported by Wuhan Institute of Physics and Mathematics, Chinese Academy of Sciences.

Appendix 1

The Lorentz matrix between the lab frame and the Sun-centered frame is

$$\Lambda=\begin{pmatrix} 1 & -\beta^1 & -\beta^2 & -\beta^3 \\ -(R\cdot\beta)^1 & R^{11} & R^{12} & R^{13} \\ -(R\cdot\beta)^2 & R^{21} & R^{22} & R^{23} \\ -(R\cdot\beta)^3 & R^{31} & R^{32} & R^{33} \end{pmatrix} \tag{A-1}$$

where R is the rotation matrix, and β is the relative velocity of the lab with respect to the Sun-centered frame.

$$R=\begin{pmatrix} \cos\chi\cos\omega_\oplus T_\oplus & \cos\chi\sin\omega_\oplus T_\oplus & -\sin\chi \\ -\sin\omega_\oplus T_\oplus & \cos\omega_\oplus T_\oplus & 0 \\ \sin\chi\cos\omega_\oplus T_\oplus & \sin\chi\sin\omega_\oplus T_\oplus & \cos\chi \end{pmatrix} \tag{A-2}$$

$$\beta=\beta_\oplus\begin{pmatrix} \sin\Omega_\oplus T \\ -\cos\eta\cos\Omega_\oplus T \\ -\sin\eta\cos\Omega_\oplus T \end{pmatrix}+\beta_L\begin{pmatrix} -\sin\omega_\oplus T_\oplus \\ \cos\omega_\oplus T_\oplus \\ 0 \end{pmatrix} \tag{A-3}$$

χ is the latitude of the laboratory. η=23°26′ is the angle between the XY celestial equatorial plane and the Earth's orbital plane. The first and the second terms on the right-hand side of Eq. (A-3) are the orbital and rotational speeds (β: linear, ω and Ω: angular) of the Earth, respectively. $T_\oplus$ starts when the y axis of the lab frame coincides with the Y axis of the Sun-centered frame, thus having a constant difference with T.

Appendix 2

As shown in Eq. (21), the shift of the resonant frequency due to various Lorentz-violating tensors can be expanded around the angular frequencies of the Earth's rotation and orbit. The following expressions give the explicit forms of the fitting parameters in Eq. (21), which absorb the rotational dependence. In these expressions, $B_q = B_{11} - B_{12}$ and $c^{(IJ)} = \dfrac{c^{IJ}+c^{JI}}{2}$.

$$\begin{aligned} A_0 = {} & \frac{1}{16}[(-6B_{11}-10B_{12})(c^{XX}+c^{YY}) \\ & -(4B_{11}+12B_{12})c^{ZZ}-(\tilde\kappa_{e-})^{ZZ}-16\kappa_{tr} \\ & +\cos 2\chi(6B_q c^{ZZ}-3(\tilde\kappa_{e-})^{ZZ})]+\frac{1}{8}\beta_\oplus[26B_{12}c^{(TX)} \\ & +14B_{11}c^{(TX)}-11(\tilde\kappa_{o+})^{YZ}-\cos 2\chi(-2B_q c^{(TX)} \\ & +(\tilde\kappa_{o+})^{YZ})]\sin\Omega_\oplus T+\frac{1}{8}\beta_\oplus[\sin\eta(-(12B_{11} \\ & +8B_{12})c^{(TZ)}+10(\tilde\kappa_{o+})^{XY})+\cos\eta(-(14B_{11} \\ & +26B_{12})c^{(TY)}-11(\tilde\kappa_{o+})^{XZ})-\cos 2\chi(\sin\eta \\ & (-4B_q c^{(TZ)}+2(\tilde\kappa_{o+})^{XY})+\cos\eta(2B_q c^{(TY)} \\ & +2(\tilde\kappa_{o+})^{XZ}))]\cos\Omega_\oplus T \end{aligned}$$

$$\begin{aligned} A_{s1} = {} & \frac{1}{4}[\beta_L(-8B_{11}c^{(TX)}-12B_{12}c^{(TX)}+6(\tilde\kappa_{o+})^{YZ}) \\ & -\sin 2\chi(-2B_q c^{(YZ)}+(\tilde\kappa_{e-})^{YZ})] \\ & +\frac{1}{4}\beta_\oplus\sin 2\chi[\sin\eta(2B_q c^{(TY)}+(\tilde\kappa_{o+})^{XZ}) \end{aligned}$$

$$+\cos\eta(2B_qc^{(TZ)}-(\tilde{\kappa}_{o+})^{XY})]\cos\Omega_{\oplus}T$$

$$A_{c1}=\frac{1}{4}[\beta_L(8B_{11}c^{(TY)}+12B_{12}c^{(TY)}+6(\tilde{\kappa}_{o+})^{XZ})$$
$$-\sin 2\chi(-2B_qc^{(XZ)}+(\tilde{\kappa}_{e-})^{XZ})]$$
$$+\frac{1}{4}\beta_{\oplus}\sin 2\chi[-2B_qc^{(TZ)}+(\tilde{\kappa}_{o+})^{XY}]\sin\Omega_{\oplus}T$$
$$-\frac{1}{4}\beta_{\oplus}\sin\eta\sin 2\chi[-2B_qc^{(TX)}+(\tilde{\kappa}_{o+})^{YZ}]\cos\Omega_{\oplus}T$$

$$A_{s2}=-\frac{1}{4}\sin^2\chi[-2B_qc^{(XY)}+(\tilde{\kappa}_{e-})^{XY}]$$
$$-\frac{1}{4}\beta_{\oplus}\sin^2\chi[2B_qc^{(TY)}+(\tilde{\kappa}_{o+})^{XZ}]\sin\Omega_{\oplus}T$$
$$-\frac{1}{4}\beta_{\oplus}\cos\eta\sin^2\chi[-2B_qc^{(TX)}+(\tilde{\kappa}_{o+})^{YZ}]\cos\Omega_{\oplus}T$$

$$A_{c2}=\frac{1}{8}\sin^2\chi[2B_q(c^{XX}-c^{YY})-(\tilde{\kappa}_{e-})^{XX}+(\tilde{\kappa}_{e-})^{YY}]$$
$$+\frac{1}{4}\beta_{\oplus}\sin^2\chi[-2B_qc^{(TX)}+(\tilde{\kappa}_{o+})^{YZ}]\sin\Omega_{\oplus}T$$
$$-\frac{1}{4}\beta_{\oplus}\cos\eta\sin^2\chi[2B_qc^{(TY)}+(\tilde{\kappa}_{o+})^{XZ}]\cos\Omega_{\oplus}T \quad \text{(A-4)}$$

$$B_0=B_{s1}=B_{c1}=B_{s2}=B_{c2}=0$$
$$C_0=C_{s1}=C_{c1}=C_{s2}=C_{c2}=0$$

$$D_0=\frac{1}{2}\beta_L\sin\chi(2B_qc^{ZT}+(\tilde{\kappa}_{o+})^{ZT})$$
$$-\frac{1}{2}B_q\beta_{\oplus}\cos\chi(c^{TY}-c^{YT})\sin\Omega_{\oplus}T$$
$$-\frac{1}{2}B_q\beta_{\oplus}\cos\eta\cos\chi(c^{TX}-c^{XT})\cos\Omega_{\oplus}T$$

$$D_{s1}=\frac{1}{2}\beta_L\cos\chi(-2B_qc^{YT}+(\tilde{\kappa}_{o+})^{XZ})$$
$$+\frac{1}{2}\sin\chi(2B_qc^{(XZ)}+(\tilde{\kappa}_{e-})^{XZ})$$
$$-\frac{1}{2}\beta_{\oplus}\sin\chi(2B_qc^{ZT}+(\tilde{\kappa}_{o+})^{XY})\sin\Omega_{\oplus}T$$
$$+\frac{1}{2}\beta_{\oplus}\sin\eta\sin\chi(2B_qc^{TX}+(\tilde{\kappa}_{o+})^{YZ})\cos\Omega_{\oplus}T$$

$$D_{c1}=-\frac{1}{2}\beta_L\cos\chi(2B_qc^{XT}+(\tilde{\kappa}_{o+})^{YZ})$$
$$-\frac{1}{2}\sin\chi(2B_qc^{(YZ)}+(\tilde{\kappa}_{e-})^{YZ})$$
$$-\frac{1}{2}\beta_{\oplus}\sin\chi[(2B_qc^{TY}-(\tilde{\kappa}_{o+})^{XZ})\sin\eta$$
$$+(2B_qc^{ZT}+(\tilde{\kappa}_{o+})^{XY})\cos\eta]\cos\Omega_{\oplus}T$$

$$D_{s2}=-\frac{1}{4}\cos\chi[2B_q(c^{XX}-c^{YY})$$
$$+(\tilde{\kappa}_{o+})^{XX}-(\tilde{\kappa}_{o+})^{YY}]$$
$$+\frac{1}{2}\beta_{\oplus}\cos\chi(2B_qc^{(TX)}+(\tilde{\kappa}_{o+})^{YZ})\sin\Omega_{\oplus}T$$
$$+\frac{1}{2}\beta_{\oplus}\cos\eta\cos\chi(2B_qc^{(TY)}-(\tilde{\kappa}_{o+})^{XZ})\cos\Omega_{\oplus}T$$

$$D_{c2}=\frac{1}{2}\cos\chi[2B_qc^{(XY)}+(\tilde{\kappa}_{e-})^{XY}]$$
$$-\frac{1}{2}\beta_{\oplus}\cos\chi(2B_qc^{(TY)}-(\tilde{\kappa}_{o+})^{XZ})\sin\Omega_{\oplus}T$$
$$+\frac{1}{2}\beta_{\oplus}\cos\eta\cos\chi(2B_qc^{(TX)}+(\tilde{\kappa}_{o+})^{YZ})\cos\Omega_{\oplus}T$$

$$E_0=\frac{1}{4}B_q\sin^2\chi(c^{XX}+c^{YY}-2c^{ZZ})$$
$$+\frac{3}{8}\sin^2\chi(\tilde{\kappa}_{e-})^{ZZ}-\frac{1}{4}\beta_{\oplus}\sin^2\chi(2B_qc^{(TX)}$$
$$+(\tilde{\kappa}_{o+})^{YZ})\sin\Omega_{\oplus}T$$
$$+\frac{1}{4}\beta_{\oplus}\sin^2\chi[-2(2B_qc^{(TZ)}-(\tilde{\kappa}_{o+})^{XY})\sin\eta$$
$$+(2B_qc^{(TY)}+(\tilde{\kappa}_{o+})^{XZ})\cos\eta]\cos\Omega_{\oplus}T$$

$$E_{s1}=\frac{1}{2}\beta_L(2B_qc^{(TX)}-(\tilde{\kappa}_{o+})^{YZ})$$
$$+\frac{1}{4}\sin 2\chi(2B_qc^{(YZ)}-(\tilde{\kappa}_{e-})^{YZ})$$
$$+\frac{1}{4}\beta_{\oplus}\sin 2\chi[(2B_qc^{(TY)}+(\tilde{\kappa}_{o+})^{XZ})\sin\eta$$
$$+(2B_qc^{(TZ)}+(\tilde{\kappa}_{o+})^{XY})\cos\eta]\cos\Omega_{\oplus}T$$

$$E_{c1}=-\frac{1}{2}\beta_L(2B_qc^{(TY)}+(\tilde{\kappa}_{o+})^{XZ})$$
$$+\frac{1}{4}\sin 2\chi(2B_qc^{(XZ)}-(\tilde{\kappa}_{e-})^{XZ})$$
$$-\frac{1}{4}\beta_{\oplus}\sin 2\chi(2B_qc^{(TZ)}-(\tilde{\kappa}_{o+})^{XY})\sin\Omega_{\oplus}T$$
$$+\frac{1}{4}\beta_{\oplus}\sin\eta\sin 2\chi(2B_qc^{(TX)}$$
$$-(\tilde{\kappa}_{o+})^{YZ})\cos\Omega_{\oplus}T$$

$$E_{s2}=-\frac{1}{8}(3+\cos 2\chi)(2B_qc^{(XY)}-(\tilde{\kappa}_{e-})^{XY})$$
$$+\frac{1}{8}\beta_{\oplus}(3+\cos 2\chi)(2B_qc^{(TY)}$$
$$+(\tilde{\kappa}_{o+})^{XZ})\sin\Omega_{\oplus}T-\frac{1}{8}\beta_{\oplus}\cos\eta(3+\cos 2\chi)$$
$$(2B_qc^{(TX)}-(\tilde{\kappa}_{o+})^{YZ})\cos\Omega_{\oplus}T$$

$$E_{c2}=\frac{1}{16}(3+\cos 2\chi)[-2B_q(c^{XX}-c^{YY})$$
$$+(\tilde{\kappa}_{e-})^{XX}-(\tilde{\kappa}_{e-})^{YY}]$$
$$+\frac{1}{8}\beta_{\oplus}(3+\cos 2\chi)(2B_qc^{(TX)}-(\tilde{\kappa}_{o+})^{YZ})\sin\Omega_{\oplus}T$$
$$+\frac{1}{8}\beta_{\oplus}\cos\eta(3+\cos 2\chi)(2B_qc^{(TY)}$$
$$+(\tilde{\kappa}_{o+})^{XZ})\cos\Omega_{\oplus}T \quad \text{(A-5)}$$

References

1. V. A. Kostelecký and S. Samuel, Phys. Rev. D, 1989, 39: 683
2. V. A. Kostelecký and R. Potting, Nucl. Phys. B, 1991, 359: 545
3. V. A. Kostelecký and S. Samuel, Phys. Rev. Lett., 1991, 66: 1811
4. V. A. Kostelecký and R. Potting, Phys. Lett. B, 1996, 381: 89
5. R. Gambini and J. Pullin, Phys. Rev. D, 1999, 59: 124021
6. J. Alfaro, H. A. Morales-T'ecotl, and L. F. Urrutia, Phys. Rev. D, 2002, 66: 124006
7. R. Bluhm, Lect. Notes. Phys., 2006, 702: 191
8. D. Colladay and V. A. Kostelecký, Phys. Rev. D, 1997, 55: 6760
9. D. Colladay and V. A. Kostelecký, Phys. Rev. D, 1998, 58: 116002
10. P. L. Stanwix, M. E. Tobar, P. Wolf, M. Susli, C. R. Locke, E. N. Ivanov, J. Winterflood, and F. van Kann, Phys. Rev. Lett., 2005, 95: 040404
11. A. Brillet and J. L. Hall, Phys. Rev. Lett., 1979, 42: 549
12. V. A. Kosteleck and M. Mewes, Phys. Rev. D, 2002, 66: 056005
13. H. Müler,C. Braxmaier, S. Herrmann, A. Peters, and C. Lämerzahl, Phys. Rev. D, 2003, 67: 056006
14. H. Müler, S. Herrmann, A. Saenz, A. Peters, and C. Lämerzahl, Phys. Rev. D, 2003, 68: 116006
15. H. Müler, Phys. Rev. D, 2005, 71: 045004
16. R. Bluhm, V. A. Kostelecký, and N. Russell, Phys. Rev. Lett., 1997, 79: 1432
17. G. Gabrielse, A. Khabbaz, D. S. Hall, C. Heimann, H. Kalinowsky, and W. Jhe, Phys. Rev. Lett., 1999, 82: 3198
18. R. K. Mittleman, I. I. Ioannou, H. G. Dehmelt, and N. Russell, Phys. Rev. Lett., 1999, 83: 2116
19. H. G. Dehmelt, R. Mittleman, R. S. Van Dyck Jr., and P. Schwinberg, Phys. Rev. Lett., 1999, 83: 4694
20. R. Jackiw and V. A. Kostelecký, Phys. Rev. Lett., 1999, 82: 3572
21. M. Pérez-Victoria, Phys. Rev. Lett., 1999, 83: 2518
22. D. Bear, R. E. Stoner, R. L. Walsworth, V. A. Kostelecky, and C. D. Lane, Phys. Rev. Lett., 2000, 85: 5038
23. R. Bluhm, V. A. Kostelecký, and N. Russell, Phys. Rev. Lett., 1999, 82: 2254
24. R. Bluhm, V. A. Kostelecký, and C. D. Lane, Phys. Rev. Lett., 2000, 84: 1098
25. V. Barger, S. Pakvasa, T. Weiler, and K. Whisnant, Phys. Rev. Lett., 2000, 85: 5055
26. O. Bertolami, D. Colladay, A.V. Kostelecky, and R. Potting, Phys. Lett. B, 1997, 395: 178
27. S. Coleman and S. L. Glashow, Phys. Rev. D, 1999, 59: 116008
28. O. Bertolami and C. S. Carvalho, Phys. Rev. D, 2000, 61: 103002